J. de Moura, J. Novo, M. Ortega, N. Barreira and M. G. Penedo, "Automated Segmentation of the Central Serous Chorioretinopathy fluid regions using Optical Coherence Tomography Scans," 2021 IEEE 34th International Symposium on Computer-Based Medical Systems (CBMS), Aveiro, Portugal, 2021, pp. 1-6, doi: 10.1109/CBMS52027.2021.00008.

Link to published version: https://doi.org/10.1109/CBMS52027.2021.00008

Automated Segmentation of the Central Serous Chorioretinopathy fluid regions using Optical Coherence Tomography Scans

Joaquim de Moura*†, Jorge Novo*†, Marcos Ortega*†, Noelia Barreira*† and Manuel G. Penedo*†
*Centro de investigación CITIC, Universidade da Coruña, Campus de Elviña, s/n, 15008 A Coruña, Spain
† Grupo VARPA, Instituto de Investigación Biomédica de A Coruña (INIBIC),
Universidade da Coruña, Xubias de Arriba, 84, 15006 A Coruña, Spain
Email: {joaquim.demoura, jnovo, mortega, nbarreira, mgpenedo}@udc.es

***Abstract*—Central serous chorioretinopathy is one of the most frequent causes of vision impairment among middle-aged adults. Optical Coherence Tomography (OCT) is a non-invasive diagnostic technique that is commonly used for the monitoring of this relevant eye disease. In this context, this paper proposes a fully automatic system for the characterization of intraretinal pathological fluid regions associated with central serous chorioretinopathy using OCT scans. To achieve this, we adapted an end-to-end fully convolutional architecture for semantic pixel-wise segmentation. The proposed methodology was tested using a heterogeneous set of 100 OCT scans of different patients. Satisfactory results were obtained, reaching values of 0.9954 ± 0.0007, 0.8792 ± 0.0079 and 0.9651 ± 0.0041 for the mean Accuracy, mean Jaccard index and mean Dice coefficient, respectively. The proposed system also demonstrated its competitive performance with respect to other state-of-the-art approaches.**

***Index Terms*—Computer-aided diagnosis, retinal imaging, optical coherence tomography, central serous chorioretinopathy, segmentation**

I. INTRODUCTION

Central serous chorioretinopathy, the fourth most frequent encountered non-surgical retinopathy, is a posterior segment disorder characterized by the serous detachment of the neurosensory retina that is associated with leakage of fluid from the choriocapillaris through the retinal pigment epithelium surface [1]. This relevant eye disease is a common cause of visual impairment among young and middle-aged adults worldwide, being more frequent in men than women [2].

Nowadays, the diagnosis and monitoring processes of patients with central serous chorioretinopathy disease are performed through the visual inspection of Optical Coherence Tomography (OCT) scans [3]. Hence, OCT constitutes a non-invasive optical imaging modality that allows the acquisition of cross-sectional tomographic scans in real-time [4]. This acquisition technique offers a micrometer-level resolution that allows a complete visualization of the main ocular tissues [5]. In Fig. 1, we can observe representative examples of OCT scans that were taken from patients with and without central serous chorioretinopathy disease, where we can observe an abnormal leakage of fluid from the choriocapillaris in the central macular region.

In daily clinical practice, the diagnosis and monitoring processes of patients with central serous chorioretinopathy disease are performed through the visual inspection of several OCT scans by the clinicians, a process which is extremely tedious and time-consuming [3]. For that reason, a fully automatic system for the characterization of intraretinal pathological fluid regions associated with the central serous chorioretinopathy using OCT scans is significantly helpful, reducing drasticaly the load of work.

Given the potential of the OCT image modality, over the recent years, different computational proposals were presented related to the automatic segmentation of intraretinal fluid regions using OCT scans over a disparity of diseases. Some examples of that can be found in the work of Roy *et al.* [6], using a end-to-end fully convolutional architecture called ReLayNet; Lee *et al.* [7] with a Convolutional Neural Network (CNN); Moura *et al.* [8] using different image processing techniques; Vidal *et al.* [9] using a machine learning strategy combined with enhanced heat maps; Girish *et al.* [10] using a Fully Convolutional Network (FCN) that was adapted by the U-Net [11] architecture; Samagaio *et al.* [12] combining different image processing and machine learning strategies to characterize different types of macular edemas; Wu *et al.* [13] with a strategy based on the maximum flow optimization algorithm combined with the probability map that was generated by a random forest classification; and Gao *et al.* [14] using multi-level feature representations and area-constraint fully convolutional network. Rao *et al.* [15] proposed a automatic segmentation of sub-retinal fluid regions in OCT scans using a deep learning strategy.

This research was funded by Instituto de Salud Carlos III, Government of Spain, DTS18/00136 research project; Ministerio de Ciencia e Innovación y Universidades, Government of Spain, RTI2018-095894-B-I00 research project; Ministerio de Ciencia e Innovación, Government of Spain through the research project with reference PID2019-108435RB-I00; Consellería de Cultura, Educación e Universidade, Xunta de Galicia, Grupos de Referencia Competitiva, grant ref. ED431C 2020/24; Axencia Galega de Innovación (GAIN), Xunta de Galicia, grant ref. IN845D 2020/38; CITIC, Centro de Investigación de Galicia ref. ED431G 2019/01, receives financial support from Consellería de Educación, Universidade e Formación Profesional, Xunta de Galicia, through the ERDF (80%) and Secretaría Xeral de Universidades (20%).

2372-9198/21/$31.00 ©2021 IEEE
DOI 10.1109/CBMS52027.2021.00008

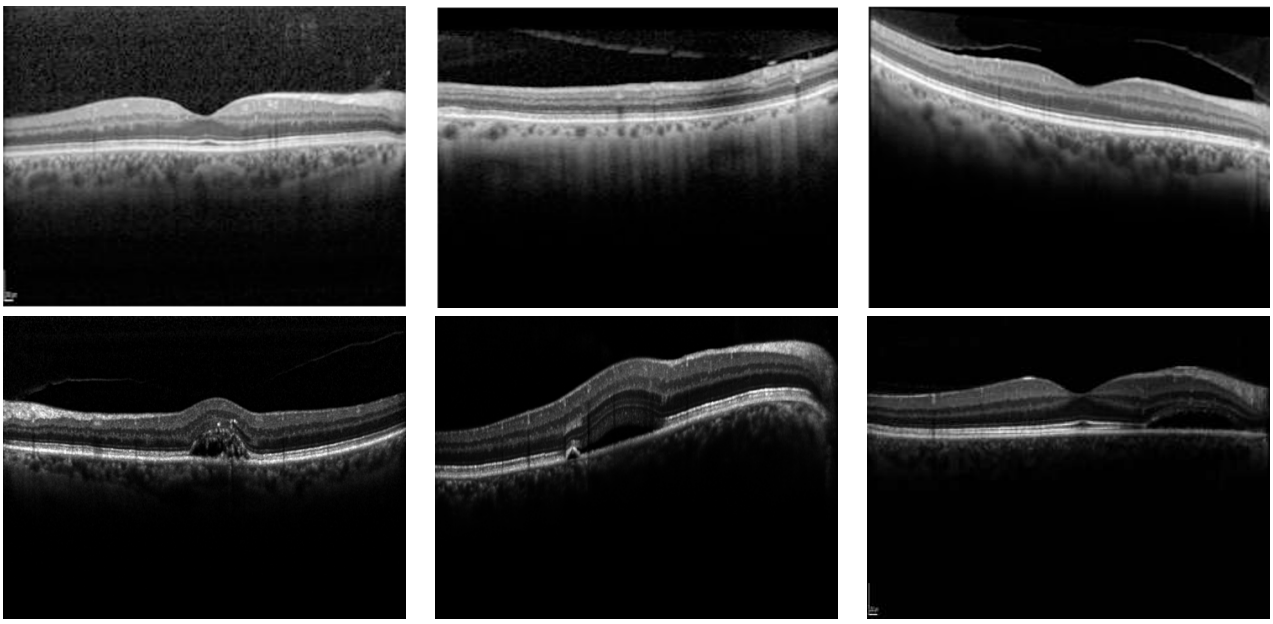

Fig. 1. Representative examples of OCT images. 1^{st} row, OCT images without the presence of central serous chorioretinopathy. 2^{nd} row, OCT images with the presence of central serous chorioretinopathy.

Despite the satisfactory results obtained by these works, most of them only address the segmentation of intraretinal fluid regions in patients with diabetic macular edema or age-related macular degeneration. In this work, we propose an end-to-end fully automatic system for the characterization of intraretinal pathological fluid regions associated with the central serous chorioretinopathy using OCT scans, an ophthalmic image modality that is increasing in popularity and clinical use. To achieve this, we adapted to this issue a fully convolutional neural network architecture for semantic pixel-wise segmentation with a great potential. Additionally, the proposed system graphically presents the results of the segmented pathological regions, facilitating the posterior analysis and diagnosis of the patients by the clinical experts.

This paper is organized as follows: Section II describes the materials and methods that were used in this research work. Results and discussions are presented and discussed in Section III, respectively. Finally, Section IV shows the most relevant conclusions of the work as well as the presentation of future lines of research.

II. MATERIALS AND METHODS

A. Network Architecture

Deep learning architectures are widely used in the field of medical imaging, commonly demonstrating superiority in both terms of time efficiency and prediction accuracy. In this work, we use a neural network architecture inspired by SegNet [16], given its simplicity, computational performance and adequate results for many relevant image segmentation issues [17]–[19]. In addition, SegNet architecture presents reduced memory requirements in comparison with other architectures during both the training and test stages and, consequently, the resulting model size is much smaller than those obtained from other architectures such as FCN, U-NET or DeconvNet. This network architecture is composed by an encoder and a corresponding decoder structures, followed by a final pixel-wise classification layer, as illustrated in Figure 2. In particular, the encoder block contains of 13 convolutional layers which correspond to the first 13 convolutional layers in the VGG-16 architecture [20]. In the case of the decoder part, the main role is to project the discriminatory semantic features learned by the encoder. Specifically, the decoder structure uses pooling indexes that are calculated in the pooling layers of the corresponding encoder to perform a non-linear up-sampling, generating a map of pixel-wise probabilities belonging to each class. Finally, the feature map of the final decoder layer is processed by the Softmax classification layer in the final pixel-wise classification between both the pathological and non-pathological regions, ensuring a well-behaved probability distribution function.

B. Training

Regarding the training stage, the used OCT image dataset was randomly divided into 2 smaller datasets, with 60% of cases for training and the remaining 40% for testing. The SegNet architecture was training using the Stochastic Gradient Descent with Momentum (SGDM) optimizer [21] with a constant learning rate of 0.001, a first-order momentum of 0.5 and a mini-batch size of 5. To correctly assess the feasibility of the problem, we follow a 10-fold cross-validation approach, where 10 repetitions with different training-test splits are performed, being calculated the mean accuracy and the mean

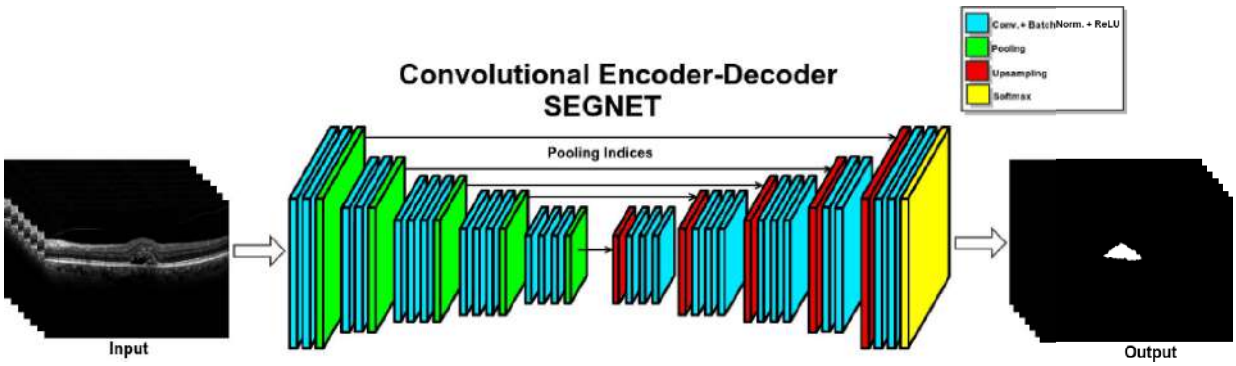

Fig. 2. An illustration of the SegNet architecture that was adapted for the experiments of this work. The encoder block consists of 13 convolutional layers which correspond to the first 13 convolutional layers in the VGG-16 architecture. The feature map of the final decoder layer is processed by the Softmax classification layer in the final pixel-wise classification between both the pathological and non-pathological classes.

cross-entropy loss [22] to illustrate the overall performance of the proposed system, as Eq. 1 establishes:

$$L = -Y \cdot log(\hat{Y}) \tag{1}$$

where Y represents the ground truth values and $\hat{Y}$ represents the estimated values for each identified category. Additionally, in order to mitigate the issue of class unbalance that is typical in this segmentation issue, we used the median frequency balancing [16] where the weight assigned each class (pathological and non-pathological) is the corresponding inverse class frequency multiplied by the median of all class frequencies in the entire OCT dataset, according to Eq. 2:

$$\omega_c = \frac{median(f(c))}{f(c)} \tag{2}$$

where $f(c)$ is the number of pixels of class c divided by the total number of pixels in OCT images where c is present, and $median(f(c))$ is the median of all frequencies.

C. Data Augmentation

Data augmentation is a popular technique widely used in deep learning strategies to reduce overfitting and make the models more robust, being especially useful for small datasets [23], [24]. In this work, we apply different combinations of affine image transformations to increase only the training data and improve the performance of the network architecture for segmentation of pathological fluid regions associated with the central serous chorioretinopathy using OCT scans. In particular, we generated a set of random values for scaling in the range [0.5, 1], rotation in the range [0, 180] degrees, and rigid translation in the range [-10 10] along the horizontal and vertical direction.

D. Dataset

The proposed method was validated using a heterogeneous image dataset that was specifically designed for the study of this relevant eye disease. In particular, the proposed dataset is composed of 100 OCT scans from 100 different patients, being 15 healthy and 85 pathological patients diagnosed with central serous chorioretinopathy. These scans were taken with a confocal scanning laser ophthalmoscope coupled with an SD-OCT device (Spectralis, Heidelberg Engineering). The OCT scans are centered on the macula, from both left and right eyes with a variability of configurations using 1-Line and the 7-Line pre-set scan protocols. All scans were manually labeled by an expert, precisely segmenting all the existing target pathological fluid regions. The study was approved by the local ethics committee and complied with the principles of the Declaration of Helsinki.

E. Evaluation

In order to quantitatively evaluate whether the trained model has generally learned about the domain, an analysis of their capability for fluid region segmentation was performed. In this way, the proposed method was evaluated using statistics that are commonly used in the state of the art to measure the performance of computational proposals in similar segmentation tasks. Thus, Accuracy, Jaccard index and Dice similarity coefficient (Eqs. 3, 4 and 5, respectively) were calculated for the quantitative validation of the segmentation results. These measures use as reference the True Positives (TP), False Positives (FP), True Negatives (TN), and False Negatives (FN):

$$\text{Accuracy} = \frac{TP + TN}{TP + TN + FP + FN} \tag{3}$$

$$\text{Jaccard} = \frac{TP}{TP + FP + FN} \tag{4}$$

$$\text{Dice} = \frac{2 \times TP}{2 \times TP + FP + FN} \tag{5}$$

III. RESULTS AND DISCUSSION

To correctly assess the suitability of the proposed system, we follow a 10-fold cross-validation approach, where 10 independent repetitions with different training-test splits were performed. Furthermore, after 100 epochs, the training stage was stopped due to the absence of further improvement in

both accuracy and cross-entropy loss. Figure 3 shows the performance that was obtained from the deep learning-based model over the repetitions of the training stage. As we can see, our model reaches stability after 10 epochs, with a best mean accuracy of 0.9965 ± 0.0001 in the epoch 99. Complementary, in Fig. 4, we can observe a similar behavior with the cross-entropy loss, demonstrating that our model presents a significative generalization capability with an excellent and stable classification performance.

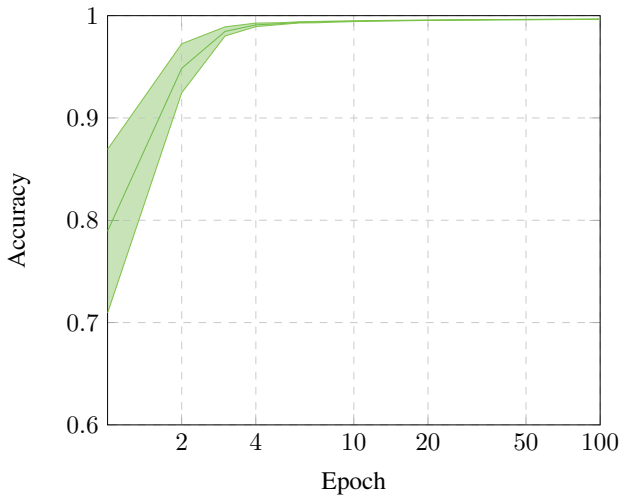

Fig. 3. Mean $\pm$ standard deviation training accuracy after the 10 independent repetitions. A logarithmic scale has been set to correctly display the values for a better understanding of the results.

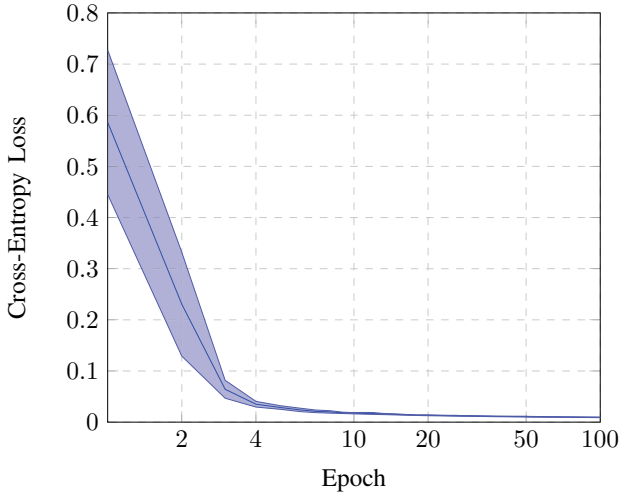

Fig. 4. Mean $\pm$ standard deviation training cross-entropy loss after the 10 independent repetitions. A logarithmic scale has been set to correctly display the values for a better understanding of the results.

Table I summarizes the results of the proposed system in terms of analysis of Accuracy, Jaccard index and Dice similarity coefficient. In particular, we present the results that were obtained in the test stage with OCT scans of patients with pathological and non-pathological conditions. In general, as we can see, satisfactory results were achieved, with a global Accuracy of 0.9954 ± 0.0007, a global Jaccard index of 0.8792 ± 0.0079 and a global Dice coefficient of 0.9651 ± 0.0041, demonstrating the robustness of the proposed system.

As illustration, Fig. 5 presents different examples of complex pathological intraretinal fluid regions that were correctly identified and characterized. As we can see, our method presents a satisfactory segmentation performance and an intuitive graphical representation that can help the ophthalmologists to produce more precise diagnosis and appropriate treatments of this relevant eye fundus disease.

Despite the satisfactory results that were obtained, the method presents some intrinsic limitations due to the complex characteristics that may be produced by this relevant eye disease in the OCT scans. In particular, some cases of misclassified pathological fluid regions wich were originated by a poor contrast, the significant levels of noise that are characteristic of this image modality or the projection of shadows derived by the retinal vascularity (Figure 6, 1^{st} row). Other times, the presence of small artifacts that are typically found in the OCT scans generates patterns of intensities with an appearance similar to those of the subretinal fluid regions (Figure 6, 2^{nd} row).

In addition, we compared our method with the few proposals of the literature that were proposed for the segmentation of intraretinal pathological fluid regions associated with the central serous chorioretinopathy, previously presented in Section I. Table II presents the best Dice similarity coefficient results of the proposed method compared to the other state-of-the-art proposals. As we can see, our end-to-end method offers a competitive performance without pre-processing or post-processing stages, outperforming the rest of the strategies, despite that these proposals were validated using OCT images that were acquired using different settings and, therefore, presenting different image characteristics, such as axial pixel-level resolution, lateral pixel-level resolution, imaging depth, bit frame rate, etc.

IV. CONCLUSIONS

In this work, we propose an end-to-end methodology for the automatic identification and segmentation of intraretinal fluid regions in OCT scans that are associated with the central serous chorioretinopathy disease. To achieve this, we adapted a fully convolutional architecture inspired by SegNet neural network with a great potential, omitting any pre-processing or post-processing stage. Additionally, the proposed system graphically presents the results of the segmented regions, characterizing them between pathological and non-pathological regions. In this way, this fully automatic system provides crucial information that facilitates a more complete analysis of the clinical expert allowing, therefore, more accurate early diagnosis of this relevant disease.

TABLE I

ACCURACY, JACCARD INDEX AND DICE SIMILARITY COEFFICIENT OF THE TEST STAGE FROM PATIENTS WITH PATHOLOGICAL AND NON-PATHOLOGICAL CONDITIONS AFTER 10 INDEPENDENT EXPERIMENTS. THE OBTAINED RESULTS ARE PRESENTED IN TERMS OF MEAN ± STANDARD DEVIATION IN PIXELS.

	Accuracy	**Jaccard**	**Dice**
Healthy	0.9967 ± 0.0001	0.9967 ± 0.0001	0.9912 ± 0.0010
Pathological	0.9942 ± 0.0015	0.7618 ± 0.0157	0.9238 ± 0.0076
Global	0.9954 ± 0.0007	0.8792 ± 0.0079	0.9651 ± 0.0041

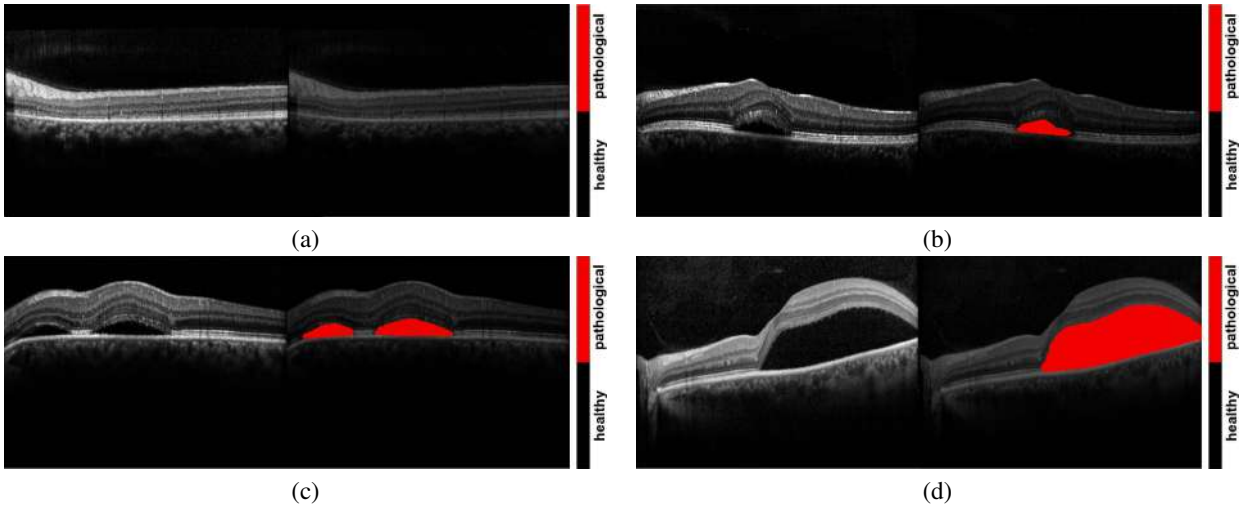

Fig. 5. Representative examples of segmentation and characterization of intraretinal fluid regions in OCT scans. (a) Extraction of the intraretinal fluid segmentation method in OCT scans from a healthy patient. (b), (c) & (d) Extractions of the intraretinal fluid segmentation method in OCT scans from patients with central serous chorioretinopathy disease.

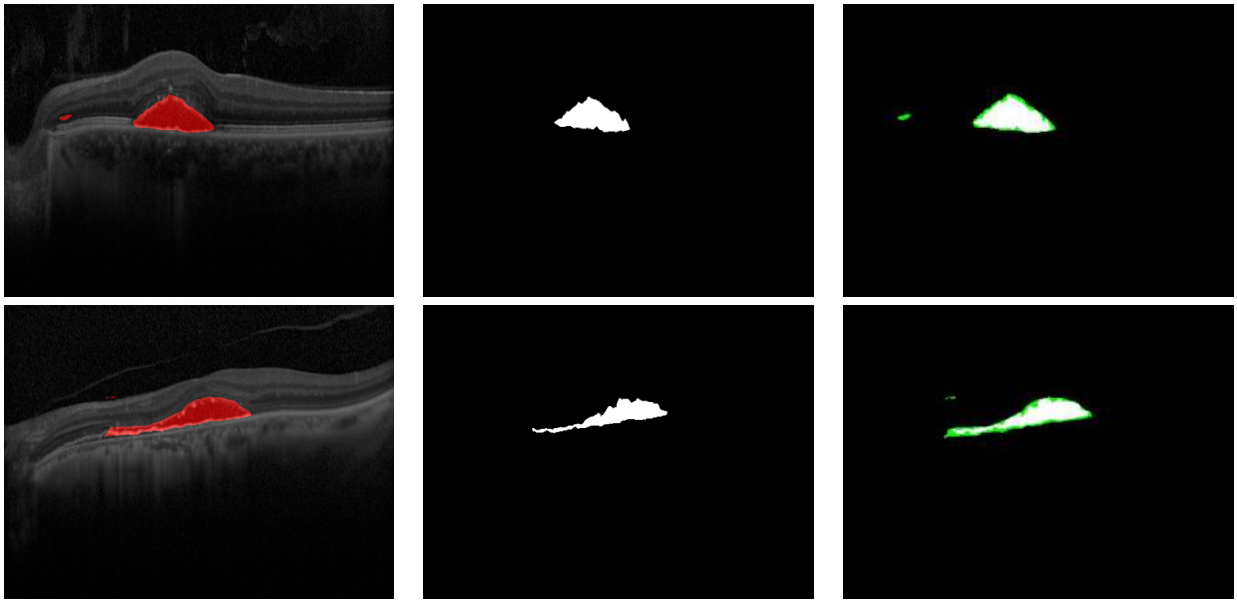

Fig. 6. Representative examples of OCT retinal images with the segmentation of intraretinal fluid regions that are associated with the central serous chorioretinopathy disease. 1^{st} column, results of the intraretinal fluid segmentation method. 2^{nd} column, manual labeling of an expert. 3^{rd} column, overlapping of the manual labeling of an expert (white) and the resulting region of intraretinal fluid segmentation (green).

TABLE II
CENTRAL SEROUS CHORIORETINOPATHY SEGMENTATION PERFORMANCE RESULTS OF THE PROPOSED METHOD COMPARED TO THE OTHER STATE-OF-THE-ART PROPOSALS.

State-of-the-art Methods	***Jaccard index***	***Dice coefficient***
(Rao, 2019) [15]	–	0.910
(Wu, 2017) [13]	–	0.934
(Gao, 2019) [14]	–	0.953
Our Method	0.8792 ± 0.0079	0.9651 ± 0.0041

Satisfactory results were obtained from the designed experiments, reaching values of 0.9954 ± 0.0007, 0.8792 ± 0.0079 and 0.9651 ± 0.0041 for the mean Accuracy, mean Jaccard index and mean Dice coefficient, respectively. Finally, the obtained results demonstrate the advantages of our proposal over the previous existing methods. In that sense, the deep encoder-decoder architecture allows to further take advantage of the potential modern deep learning algorithms. This leads to an improvement in the classification of pathological and non-pathological regions in OCT scans. As future work, we plan to extend this methodology to segment other pathological structures of the eye fundus that may be derived from many types of ocular or systemic diseases.

REFERENCES

[1] Christian Prünte and Josef Flammer, "Choroidal capillary and venous congestion in Central Serous Chorioretinopathy," *American journal of ophthalmology*, vol. 121, no. 1, pp. 26–34, 1996.

[2] Maria Wang, Inger Christine Munch, Pascal W Hasler, Christian Prünte, and Michael Larsen, "Central Serous Chorioretinopathy," *Acta ophthalmologica*, vol. 86, no. 2, pp. 126–145, 2008.

[3] George Joseph Manayath, Ratnesh Ranjan, Vanee Sheth Shah, Smita S Karandikar, Veerappan R Saravanan, and Venkatapathy Narendran, "Central Serous Chorioretinopathy: Current update on pathophysiology and multimodal imaging," *Oman journal of ophthalmology*, vol. 11, no. 2, pp. 103, 2018.

[4] David Huang, Eric A Swanson, Charles P Lin, Joel S Schuman, William G Stinson, Warren Chang, Michael R Hee, Thomas Flotte, Kenton Gregory, Carmen A Puliafito, et al., "Optical Coherence Tomography," *science*, vol. 254, no. 5035, pp. 1178–1181, 1991.

[5] Carmen A Puliafito, Michael R Hee, Charles P Lin, Elias Reichel, Joel S Schuman, Jay S Duker, Joseph A Izatt, Eric A Swanson, and James G Fujimoto, "Imaging of macular diseases with Optical Coherence Tomography," *Ophthalmology*, vol. 102, no. 2, pp. 217–229, 1995.

[6] Abhijit Guha Roy, Sailesh Conjeti, Sri Phani Krishna Karri, Debdoot Sheet, Amin Katouzian, Christian Wachinger, and Nassir Navab, "ReLayNet: retinal layer and fluid segmentation of macular Optical Coherence Tomography using fully convolutional networks," *Biomedical optics express*, vol. 8, no. 8, pp. 3627–3642, 2017.

[7] Cecilia S Lee, Ariel J Tyring, Nicolaas P Deruyter, Yue Wu, Ariel Rokem, and Aaron Y Lee, "Deep-learning based, automated segmentation of macular edema in Optical Coherence Tomography," *Biomedical optics express*, vol. 8, no. 7, pp. 3440–3448, 2017.

[8] Joaquim de Moura, Jorge Novo, Susana Penas, Marcos Ortega, Jorge Silva, and Ana Maria Mendonça, "Automatic Characterization of the Serous Retinal Detachment Associated with the Subretinal Fluid Presence in Optical Coherence Tomography Images," *Procedia Computer Science*, vol. 126, pp. 244–253, 2018.

[9] Plácido L Vidal, Joaquim de Moura, Jorge Novo, Manuel G Penedo, and Marcos Ortega, "Intraretinal fluid identification via enhanced maps using Optical Coherence Tomography images," *Biomedical optics express*, vol. 9, no. 10, pp. 4730–4754, 2018.

[10] G Girish, Bibhash Thakur, Sohini Roy Chowdhury, Abhishek R Kothari, and Jeny Rajan, "Segmentation of intra-retinal cysts from optical coherence tomography images using a fully convolutional neural network model," *IEEE journal of biomedical and health informatics*, vol. 23, no. 1, pp. 296–304, 2018.

[11] O Ronneberger, P Fischer, and TU-net Brox, "Convolutional networks for biomedical image segmentation," in *Paper presented at: International Conference on Medical Image Computing and Computer-Assisted Intervention2015*.

[12] Gabriela Samagaio, Aída Estévez, Joaquim de Moura, Jorge Novo, María Isabel Fernández, and Marcos Ortega, "Automatic macular edema identification and characterization using OCT images," *Computer methods and programs in biomedicine*, vol. 163, pp. 47–63, 2018.

[13] Menglin Wu, Wen Fan, Qiang Chen, Zhenlong Du, Xiaoli Li, Songtao Yuan, and Hyunjin Park, "Three-dimensional continuous max flow optimization-based serous retinal detachment segmentation in SD-OCT for Central Serous Chorioretinopathy," *Biomedical optics express*, vol. 8, no. 9, pp. 4257–4274, 2017.

[14] Kun Gao, Sijie Niu, Zexuan Ji, Menglin Wu, Qiang Chen, Rongbin Xu, Songtao Yuan, Wen Fan, Yuehui Chen, and Jiwen Dong, "Double-branched and area-constraint fully convolutional networks for automated serous retinal detachment segmentation in SD-OCT images," *Computer methods and programs in biomedicine*, vol. 176, pp. 69–80, 2019.

[15] TJ Narendra Rao, GN Girish, Abhishek R Kothari, and Jeny Rajan, "Deep learning based sub-retinal fluid segmentation in central serous chorioretinopathy optical coherence tomography scans," in *2019 41st Annual International Conference of the IEEE Engineering in Medicine and Biology Society (EMBC)*. IEEE, 2019, pp. 978–981.

[16] Vijay Badrinarayanan, Alex Kendall, and Roberto Cipolla, "Segnet: A deep convolutional encoder-decoder architecture for image segmentation," *IEEE transactions on pattern analysis and machine intelligence*, vol. 39, no. 12, pp. 2481–2495, 2017.

[17] Jing Tang, Jun Li, and Xiangping Xu, "Segnet-based gland segmentation from colon cancer histology images," in *2018 33rd Youth Academic Annual Conference of Chinese Association of Automation (YAC)*. IEEE, 2018, pp. 1078–1082.

[18] Pranita Pradhan, Tobias Meyer, Michael Vieth, Andreas Stallmach, Maximilian Waldner, Michael Schmitt, Juergen Popp, and Thomas Bocklitz, "Semantic Segmentation of Non-linear Multimodal Images for Disease Grading of Inflammatory Bowel Disease: A SegNet-based Application," in *International Conference on Pattern Recognition Applications and Methods 2019*, 2019.

[19] Lianyi Wu, Yiming Liu, Yelin Shi, Bin Sheng, Ping Li, Lei Bi, and Jinman Kim, "Optic Disc and Cup Segmentation Based on Enhanced SegNet," in *Proceedings of the 32nd International Conference on Computer Animation and Social Agents*, 2019, pp. 33–36.

[20] Shuying Liu and Weihong Deng, "Very deep convolutional neural network based image classification using small training sample size," in *2015 3rd IAPR Asian conference on pattern recognition (ACPR)*. IEEE, 2015, pp. 730–734.

[21] Ilya Sutskever, James Martens, George Dahl, and Geoffrey Hinton, "On the importance of initialization and momentum in deep learning," in *International conference on machine learning*, 2013, pp. 1139–1147.

[22] Zhilu Zhang and Mert Sabuncu, "Generalized cross entropy loss for training deep neural networks with noisy labels," in *Advances in neural information processing systems*, 2018, pp. 8778–8788.

[23] David A Van Dyk and Xiao-Li Meng, "The art of data augmentation," *Journal of Computational and Graphical Statistics*, vol. 10, no. 1, pp. 1–50, 2001.

[24] Zeshan Hussain, Francisco Gimenez, Darvin Yi, and Daniel Rubin, "Differential data augmentation techniques for medical imaging classification tasks," in *AMIA Annual Symposium Proceedings*. American Medical Informatics Association, 2017, vol. 2017, p. 979.